Investigation of Total Energy Density and Power Flow for Propagating Modes of Square-Core Optical Fiber

Zahra Saghi

Department of Physics, Shahid Chamran University of Ahvaz, Ahvaz, Iran

Corresponding author email: zahra.saghi74@gmail.com

ABSTRACT— **Square-core optical fiber is one of the modern optical fibers used in many fields such as astronomical spectroscopy, laser cutting and thermal applications of lasers and beam shaping optics. In this paper, an optical fiber that has a square core with a side of 55 μm is designed for propagating laser light at a wavelength of 1060 *nm*. Then, using numerical analysis by finite element method (FEM), the distribution of electric and magnetic fields with different polarizations and magnetizations is analyzed for the first three propagating modes of the optical fiber. In the following, the changes of total energy density and power flow are investigated. Finally, the results of the figures and plots are discussed completely.**

KEYWORDS: electric field, magnetic field, modes, optical fiber, power flow, total energy density.

I. INTRODUCTION

Optical fibers are used in many well-known fields such as telecommunications [1], [2], computer networks [3], [4] and medicine [5]–[7]. Also, these optical devices have many uses in sensors [8], [9], fiber lasers [10], [11], high-frequency optical scanners [12], scanning near-field optic/atomic force microscopes (SNOAM) [13], optical recording [14], measurement of the degree of coherence of light [15], optical imaging transport [16], [17], photolithography techniques [18], three-dimensional optical memory [11], sensitive detection of the refractive index [19], measurement of piezoelectric vibration [20] and others.

One of the simplest and most widely used types of optical fibers is step-index fiber. In these devices, core is surrounded by a cladding region which has the lower refractive index, satisfying inequality $n_{clad} \langle n_{core}$ [21]. This leads to the well-known total internal reflection phenomenon and the simple guided-ray picture of wave-guidance [22]. Considering the number of modes that step-index optical fibers propagate, they can be classified into two important groups: single mode and multimode step-index optical fibers. Multimode step-index optical fibers are more easily excited than single mode ones [23] and are useful in qualitative and quantitative chemical analysis [24], transmission media of optical communication systems [23], networks [25], coupling with LED [26] and other applications.

Optical fibers, in their simplest form, have a circular core on their cross-sectional area through which light is transported to the end of the fiber with minimal loss. By improving the geometrical possibilities [27], fiber optic cables in addition to laser light transmission, are an important part of system design that reduce the need for beam shaping optics [28], [29]. Therefore, depending on optical fibers applications, they are existed in different shapes, including octagonal, rectangular, square, etc [30]. Square fibers are highly multimode and perform a great deal of ray mixing during optical propagation [30]. These fibers can convert a Gaussian beam into higher-order optical orbital angular momentum (OAM) modes because of breaking the circular symmetry of the waveguide [31]. Therefore,

they can propagate both EHmn and HEmn modes that m and n refer to azimuthal and radial coordinates [31], [32]. In such a fiber, these modes are not degenerate, because square is not invariant under rotating with π/4. However, the HE modes in square-core fiber is also degenerate, since square cross section remains the same under rotation of π/2 [32]. These optical fibers can be used for works in which the shape of the beam is important and needs to be done with great precision [29]-[31]. Also, due to their square nature, these fibers couple the output of diode lasers much more efficiently [29]. Optical fibers with square cores were widely used in astronomical spectroscopy [30]. These fibers have a high potential for use in laser welding, laser cutting and other heat treatment applications because the square-formed beam treats the materials more uniformly than the circular-formed beam when it moves along the surface [29], [33]. Experimental results also show that the power of square-core optical fibers is comparable to the power of circular-core optical fibers [29]. The dispersion characteristics and in particular, the zero dispersion wavelength of the single-mode optical fibers (SMFs) fabricated with silica, were studied in the telecommunication region as the structural parameters such as the radius of the fiber core and the relative core-cladding index difference are changed before [34]. It is interesting to note that a square-core optical fiber could be beneficial from the perspective of modal behavior [27]. square-cores are somewhat analogous to round-cores in that they possess two degenerate orthogonal modes with no cut-off for the lowest order mode [27]. To the best of the author's knowledge, no one has studied in detail the modal behavior and especially the properties of the dispersion of such a square fiber.

The interaction between electromagnetic fields and the states of the glass makes it polarized and magnetized. Simulation of how electric and magnetic fields are distributed in the optical fibers, as well as predicting the amount of energy they carry in a special wavelength of the light, is very important in the process of designing of the optical fibers because of saving in fabrication costs.

As a result of light-matter interactions, an important modal characteristic includes the effective mode index, n_{eff}, which defines phase matching conditions in a number of nonlinear processes [21]. This value can be determined by computing the propagation constant in the fiber [35]. Analytical study of the square fiber modes and calculating of the electric and magnetic field functions of such fibers faces computational complexities even for the circular–core optical fiber which is the most common and simplest core shape [36].

This paper focuses on the designing a step-index square-core optical fiber as shown in Fig. 1 Then, the distribution of electric and magnetic fields is obtained by using finite element method (FEM) that is shown in Fig. 2 and Fig. 3 respectively. In the following, the plots of total energy density and power flow of the fundamental mode of this optical fiber is drawn in Fig. 4 Finally, the results of the figures and plots are explained in detail.

II. THEORETICAL METHODS

A. Physical Structure of Square-Core Optical Fiber

Optical fiber with a square core consists of a core that is covered by a cladding and a buffer coating similar to a circular-core optical fiber. In Fig. 1, the cross section of this fiber and its dimensions is shown.
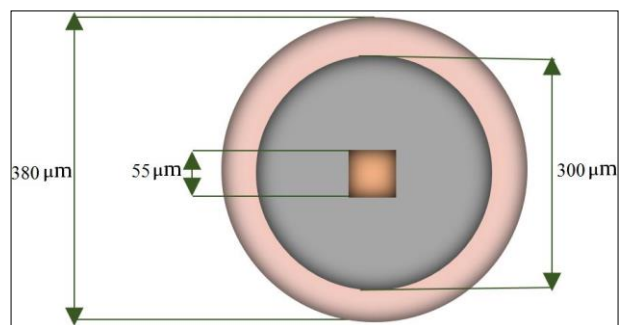

Fig. 1. The schematic diagram of the cross-sectional area and the dimensions of the core, cladding and buffer coating of the square-core optical fiber.

Due to have the step-index structure, the core of this fiber is made of doped silica with a refractive index of 1.4646, the cladding is made of undoped silica with a refractive index of 1.4572 and the buffer coating is made of a

polymer with a refractive index of 1.3827 [37]–[40]. In This work square-core optical fiber is used for propagating light with a wavelength of 1060 *nm*. This wavelength of the light is used in many fields such as single-mode diode lasers for telecommunication, industrial and medical applications [41]–[43], gain-switched laser diodes for high average power and high repetition rate [44], high-brightness edge-emitting semiconductor lasers [45], hybrid integrated tunneling diode [46], compact ultrafast reflective Fabry-Perot tunable lasers [47], cutting and skin-ablative properties of pulsed mid-infrared laser surgery [48], fiber-coupled diode lasers for material processing and pumping applications [49], ultrashort pulse fiber amplifiers [50] and others.

B. *Computing the Propagating Modes of Square-Core Optical Fiber*

The electromagnetic wave is propagated along the z direction as follows [36]

$$\mathbf{H}(x,y,z,t) = \mathbf{H}(x,y)e^{i(\omega t - kz)} \quad (1)$$

where ω is the angular frequency and k is also the propagation constant. The eigenvalue equation for the magnetic field H is derived from the Helmholtz equation as follows [36]:

$$\nabla \times (n^{-2}\nabla \times \mathbf{H}) - k^2\mathbf{H} = 0 \quad (2)$$

The magnetic field outside the optical fiber is set to be zero because the amplitude of the magnetic field is a function of the radius of the optical fiber cladding and decays rapidly when it increases [36].

As told before, analytical study of computing the propagating modes faces computational complexities. Therefore, finite element method (FEM) is used to compute the first three modes. This model is simulated for the cross section of the optical fiber in xy-plane [51]. The optical fiber effective mode index must be as follows:

$$n_{clad} \langle n_{eff} \langle n_{core} \quad (3)$$

Using the finite element method, the first three effective mode indexes is computed for the square-core optical fiber as follows:

$$\begin{cases} n_{eff_{fund}} \approx 1.4645 \\ n_{eff_2} \approx 1.4644 \\ n_{eff_3} \approx 1.4643 \end{cases} \quad (4)$$

It should be noted that the number of elements used in this simulation is so high and the maximum of the mesh size is 20 *nm* to achieve reliable numerical calculations. In the following, the electric and magnetic fields distributions for the first three modes and total energy density and power flow for fundamental mode are discussed and investigated in detail.

III. RESULTS AND DISCUSSION

A. *Distribution of Electric Field in Square-Core Optical Fiber*

Figure 2 shows that the square symmetry of the optical fiber core is very important in the distribution of the electric field profile.
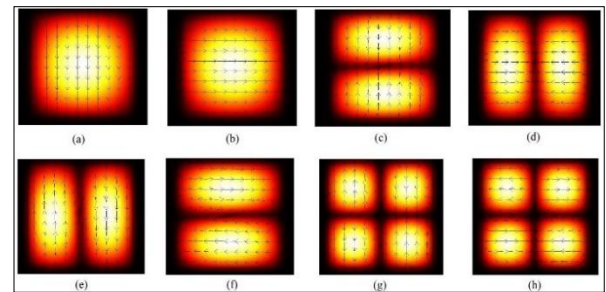

Fig. 2. The distribution of the norm of the electric field inside the optical fiber core that propagates laser light at a wavelength of 1060 nm for (a) the first and (b) second situation of the fundamental mode, (c) the first, (d) second, (e) third and (f) forth possible situation of the second mode and (g) the first and (h) second situation of the third mode with different polarizations.

The distribution of the norm of electric field for two different polarizations of the fundamental mode in Figs. 2(a) and 2(b) is almost Gaussian and for both of these cases, the electric field decreases as it moves away from the center of the core. Near the cladding, the norm of electric field reaches its minimum value in the core. In first case of the arrangement of the electric field vectors for the fundamental mode showing in

Fig. 2(a), the core of optical fiber is polarized along the y direction and acts like an electric dipole because the electric field vectors are directed from top to bottom of the core, indicating the accumulation of positive charges in the upper part of the core and the accumulation of negative charges in the lower part of it. Figure 2(b) which shows the second case of the arrangement of the electric field vectors for the fundamental mode, the core of optical fiber is polarized along the x direction and acts like an electric dipole because the electric field vectors are directed from left to right side of the core, indicating the accumulation of positive charges in the left side of the core and the accumulation of negative charges in the right side of it.

For Figs. 2(c)-2(f) which represent all situations of electric field distribution of the second mode, the core is divided in two polarized regions that in the center of the core, the norm of electric field is zero. In Fig. 2(c) which shows the first situation of the arrangement of the electric field vectors for the second mode of the fiber, the core is polarized along the y direction symmetrically and acts like two electric dipoles so that the upper and lower parts of the core are two polarized parts with different polarizations and in the upper part of the core, the upper part of this region, positive charges and the lower part of this region, negative charges have accumulated. Also, In the lower part of the core, the upper part of this region, negative charges and the lower part of this region, positive charges have accumulated. Figure 2(d) shows that in this case, the core is polarized along the x direction symmetrically and acts like two electric dipoles so that the left and right sides of the core are two polarized parts with different polarizations and in the left side of the core, the left side of this region, positive charges and the right side of this region or the middle of the core, negative charges have accumulated. Also, In the right side of the core, the right side of this region, positive charges and the left side of this region, negative charges have accumulated. For the third case of this mode which shows in Fig. 2(e), the core is polarized along the y direction symmetrically and acts like two electric dipoles so that the left and right sides of the core are

two polarized parts with different polarizations and in the left part of the core, the lower part of this region, positive charges and the upper part of this region, negative charges have accumulated. Also, In the right side of the core, the upper part of this region, positive charges and the lower part of this region, negative charges have accumulated. It is interesting to note that the electric field is zero in the direction x=0 and y=0 and the intersection of these lines inside the core. The final possible situation of the second mode of this fiber showing in Fig. 2(f), the core is polarized along the x direction symmetrically and acts like two electric dipoles so that the upper and lower parts of the core are two polarized parts with different polarizations and in the upper part of the core, the left side of this region, positive charges and the right side of this region, negative charges have accumulated. Also, In the lower part of the core, the right side of this region, positive charges and the left side of this region, negative charges have accumulated. It is interesting to note that the electric field is zero in the direction x=0 and y=0 and the intersection of these lines inside the core.

Considering two possible situations of electric field distribution of the third mode which shows in Figs. 2(g) and 2(h), the core is divided in four polarized regions that the norm of electric field is zero in the center of the core. Figure 2(g) which shows the first case of the arrangement of the electric field vectors for the third mode of this fiber, the core is polarized along the y direction symmetrically and acts like four electric dipoles so that in the left side of the upper part of the core, the middle of the left side of it positive charges and the upper part of this region, negative charges and in the left side of the lower part of the core, the middle of the left side of it positive charges and the lower part of this region, negative charges have accumulated. Also, in the right side of the upper part of the core, the middle of the right side of it negative charges and the upper part of this region, positive charges and in the right side of the lower part of the core, the middle of the right side of it negative charges and the lower part of this region, positive charges have accumulated. It is interesting to note that the electric field is

zero in the direction x=0 inside the core. In the case of the final possible situation of the third mode of this fiber which shows in Fig. 2(h), the core is polarized along the x direction symmetrically and acts like four electric dipoles so that in the left side of the upper part of the core, the middle of the upper part of it positive charges and the left side of this region, negative charges and in the left side of the lower part of the core, the middle of the lower part of it negative charges and the left side of this region, positive charges have accumulated. Also, in the right side of the upper part of the core, the middle of the upper part of it positive charges and the right side of this region, negative charges and in the right side of the lower part of the core, the middle of the lower part of it negative charges and the right side of this region, positive charges have accumulated. It is interesting to note that the electric field is zero in the direction y=0 inside the core.

B. *Distribution of Magnetic Field in Square-Core Optical Fiber*

As shown in Fig. 3, the magnetic field vectors along the z direction, by moving away from the core will be orientated in the random way which means that the magnetic field is zero inside the cladding and the buffer coating of the fiber. In Fig. 3, the orientation of magnetic field vectors obeys the transverse nature of electromagnetic waves as expected.
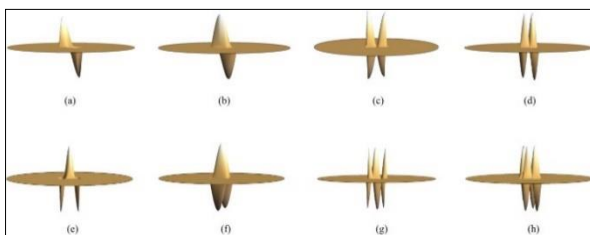

Fig. 3. The distribution of the magnetic field for the square-core optical fiber that propagates laser light at a wavelength of 1060 nm for (a) the first and (b) second situation of the fundamental mode, (c) the first, (d) second, (e) third and (f) forth possible situation of the second mode and (g) the first and (h) second situation of the third mode with different magnetizations.

For the first situation of orientation of magnetic field vectors of the fundamental mode of the fiber showing in Fig. 3(a), the core of optical fiber is magnetized along the x direction because the magnetic field vectors are directed from left to right side of the core. Here, the core acts like a magnetic dipole that the left side of the core is supposed to be the south pole and the right side of it is supposed to be the north pole of a bar magnet. Also, the magnetic field is zero in the direction x=0 inside the core. In Fig. 3(b) which shows the second possible situation of the fundamental mode, the core of optical fiber is magnetized along the y direction because the magnetic field vectors are directed from bottom to top of the core. Here, the core acts like a magnetic dipole that the lower part of the core is supposed to be the south pole and the upper part of it is supposed to be the north pole of a bar magnet. Also, the magnetic field is zero in the direction y=0 inside the core.

In Figs. 3(c)-3(f) which represent all situations of magnetic field distribution of the second mode, the core is divided in two magnetized regions. For the first case of the distribution of magnetic field for the second mode of the fiber showing in Fig. 3(c), the core of optical fiber is magnetized along the x direction symmetrically and acts like two magnetic dipoles so that the upper and lower parts of the core are two magnetized parts with different magnetizations and in the upper part of the core, the left side of this region acts like a south pole and the right side of this region behaves like a north pole of a bar magnet. Also, In the lower part of the core, the right side of this region acts like a south pole and the left side of this region behaves like a north pole of a bar magnet. It is interesting to note that the magnetic field is zero in the direction x=0 and y=0 and the intersection of these lines inside the core. This situation is similar to have two bar magnets that they are placed opposite of each other in xy-plane horizontally. Figure 3(d) that is the second possible situation of the orientation of the magnetic field vectors for the second mode shows the core of optical fiber is magnetized along the y direction symmetrically and acts like two magnetic dipoles so that the left and right parts of the core are two magnetized parts with different magnetizations and in the left side of the core, the lower part of this region acts like a south pole and the upper part of this region behaves like a north pole of a bar

magnet. Also, In the right side of the core, the upper part of this region acts like a south pole and the lower part of this region behaves like a north pole of a bar magnet. It is interesting to note that the magnetic field is zero in the direction x=0 and y=0 and the intersection of these lines inside the core. This situation is similar to have two bar magnets that they are placed opposite of each other in xy-plane vertically. The third possible case of the distribution of magnetic field vectors of the second mode showing in Fig. 3(e), the core of optical fiber is magnetized along the x direction symmetrically and acts like two magnetic dipoles so that the left and right sides of the core are two magnetized parts with different magnetizations and in the left side of the core, the left side of this region acts like a north pole and the right side of this region or the middle of the core behaves like a south pole of a bar magnet. Also, In the right side of the core, the right side acts like a north pole and the left side of this region behaves like a south pole of a bar magnet. This situation is similar to have two bar magnets that they are arranged along each other from the south pole in xy-plane horizontally. Figure 3(f), the final situation of the distribution of the magnetic field for the second mode of the fiber, shows that the core is magnetized along the y direction symmetrically and acts like two magnetic dipoles so that the top and bottom of the core are two magnetized parts with different magnetizations and in the upper part of the core, the upper part of this region acts like a north pole and the lower part of this region or the middle of the core behaves like a south pole of a bar magnet. Also, In the lower part of the core, the upper part of this region acts like a south pole and the lower part of this region behaves like a north pole of a bar magnet. This situation is similar to have two bar magnets that they are arranged along each other from the south pole in xy-plane vertically.

Considering two possible situations of magnetic field distribution of the third mode which shows in Figs. 3(g) and 3(h), the core is divided in four magnetized regions. For the first possible situation of the distribution of magnetic field vectors of the third mode which shows in Fig. 3(g), the core of optical fiber is

magnetized along the x direction symmetrically and acts like four magnetic dipoles so that in the left side of the upper part of the core, the middle of the upper part of it acts like a south pole and the left side of this region behaves like a north pole and in the left side of the lower part of the core, the middle of the lower part of it acts like a north pole and the left side of this region behaves like a south pole of a bar magnet. Also, in the right side of the upper part of the core, the middle of the upper part of it acts like a south pole and the right side of this region behaves like a north pole and in the right side of the lower part of the core, the middle of the lower part of it acts like a north pole and the right side of this region behaves like a south pole of a bar magnet. It is interesting to note that the magnetic field is zero in the direction y=0 inside the core. This situation is similar to have four bar magnets that they are arranged along each other pairwise in the top and bottom of the core from the south pole and north pole respectively in xy-plane horizontally. Figure 3(h), the final situation of the distribution of the magnetic field for the third mode of the fiber, shows that the core is magnetized along the y direction symmetrically and acts like four magnetic dipoles so that in the left side of the upper part of the core, the middle of the left side of it acts like a north pole and the upper part of this region behaves like a south pole and in the left side of the lower part of the core, the middle of the left side of it acts like a north pole and the lower part of this region behaves like a south pole of a bar magnet. Also, in the right side of the upper part of the core, the middle of the right side of it acts like a south pole and the upper part of this region behaves like a north pole and in the right side of the lower part of the core, the middle of the right side of it acts like a south pole and the lower part of this region behaves like a north pole of a bar magnet. It is interesting to note that the magnetic field is zero in the direction x=0 inside the core. This situation is similar to have four bar magnets that they are arranged along each other in the left and right side of the core pairwise from the north pole and south pole respectively in xy-plane vertically.

C. *Distribution of Total Energy Density and Power Flow in Square-Core Optical Fiber*

Figure 4 shows the total energy density and power flow plots for the fundamental mode of the square-core optical fiber which is drawn for all parts of it in terms of x and y in kPa and W/μm^2 respectively.
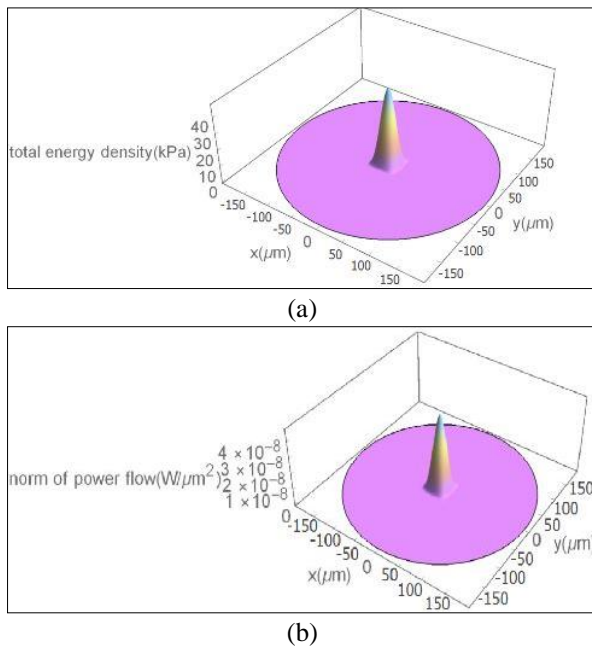

(a)

(b)

Fig. 4. The plots of (a) total energy density and (b) norm of power flow in terms of optical fiber dimensions along the x and y directions. These quantities are expressed in kPa and W/μm^2 respectively. Also, the dimensions of the optical fiber are considered in micrometers (μm).

As shown in Fig. 4(a), the maximum amount of total energy density which is concentrated in the center of the optical fiber core for the fundamental mode is 46.655 kPa. Figure 4(b) shows the biggest transfer of the power flow from the fiber region reaches a maximum of 4.666×10^{-8} W/μm^2 in the center of the core for the fundamental mode of the fiber. Also, for both of total energy density and power flow that shows in Figs. 4(a) and 4(b), the amounts of these quantities decrease rapidly when moves away from the optical fiber core and reach zero near the cladding and inside of the buffer coating as expected. Therefore, the electromagnetic waves propagate in all parts of the core for the fundamental propagating mode.

IV. CONCLUSION

In this paper, the distribution of electric and magnetic fields for all possible situations with different polarizations and magnetizations for the first three modes of the square-core optical fiber was studied using finite element method (FEM). It was also observed that the shape of the optical fiber core is very effective in the symmetry and distribution of the fields. Then, it was understood that the optical fiber core was completely polarized and magnetized in the direction of the wave propagation axis. Next, the maximum total energy density and power flow were obtained for the fundamental mode of the fiber 46.655 kPa and 4.666×10^{-8} W/μm^2 respectively. As mentioned in this work, square-core optical fiber is one of the most widely used types of modern optical fibers and the author hopes that this study is helpful for the researchers working in this field of science and technology.

REFERENCES

[1] A.G. Chynoweth, "The fiber lightguide," Phys. Today, Vol. 29, pp. 28–37, 1976.

[2] N. Niizeki, "Recent progress in glass fibers for optical communication," Jpn. J. Appl. Phys, Vol. 20, No. 8, pp. 1347-1360, 1981.

[3] A.V. Bourdine, V.A. Burdin, V. Janyani, A.K. Ghunawat, G. Singh, and A.E. Zhukov, "Design of silica multimode optical fibers with extremely enlarged core diameter for laser-based multi-gigabit short-range optical networks," Photonics, Vol. 5, No. 37, pp. 1-22, 2018.

[4] E. Rawson and R. Metcalfe, "Fibernet: Multimode optical fibers for local computer networks," IEEE. Trans. Commun, Vol. 26, No. 7, pp. 983-990, 1978.

[5] A. Katzir, Lasers and Optical Fibers in Medicine, Academic Press, 1993.

[6] G.v. Bally, E. Brune, and W. Mette, "Holographic endoscopy with gradient-index optical imaging systems and optical fibers," Appl. Optics, Vol. 25, No. 19, pp. 3425-3429, 1986.

[7] A.K. Yetisen, N. Jiang, A. Fallahi, Y. Montelongo, G.U.R-Esparza, A. Tamayol, Y.S. Zhang, I. Mahmood, S-A. Yang, K.S. Kim, H. Butt, A. Khademhosseini, and S-H. Yun, "Glucose-sensitive hydrogel optical fibers functionalized with phenylboronic acid," Adv. Mater. Vol. 29, pp. 1606380 (1-11), 2017.

[8] Z. Liu, Z.F. Zhang, H-Y. Tam, and X. Tao, "Multifunctional smart optical fibers: materials, fabrication, and sensing applications," Photonics, Vol. 6, No. 48, pp. 1-24, 2019.

[9] C. Wang and K. Shida, "A multifunctional double-fiber type distributed optical fiber sensor," Jpn. J. Appl. Phys, Vol. 46, No. 2, pp. 852-855, 2007.

[10] S. Addanki, I.S. Amiri, and P. Yupapin, "Review of optical fibers-introduction and applications in fiber lasers," Results. Phys. Vol. 10, pp. 743-750, 2018.

[11] M. Tsuji, N. Nishizawa, and Y. Kawata, "Compact and high-power mode-locked fiber laser for three-dimensional optical memory," Jpn. J. Appl. Phys, Vol. 47, pp. 5797-5799, 2008.

[12] R. Isago, S. Domae, D. Koyama, K. Nakamura, and S. Ueha, "High-frequency optical scanner based on bending vibration of optical fiber," Jpn. J. Appl. Phys, Vol. 45, No. 5B, pp. 4773-4779, 2006.

[13] N. Chiba, H. Muramatsu, T. Ataka, and M. Fujihira, "Observation of topography and optical image of optical fiber end by atomic force mode scanning near-field optical microscope," Jpn. J. Appl. Phys, Vol. 34, pp. 321-324, 1995.

[14] C-H. Tien, H-L. Chou, Y. Chiu, W. Hsu, T.D. Milster, Y-C. Lai, and H-P.D. Shieh, "Fiber-lens-based module for optical recording applications," Jpn. J. Appl. Phys, Vol. 42, pp. 4345-4348, 2003.

[15] T. Suzuki, "Interferometric uses of optical fiber," Jpn. J. Appl. Phys, Vol. 5, pp. 1065–1074, 1966.

[16] T.H. Tuan, S. Kuroyanagi, K. Nagasaka, T. Suzuki, and Y. Ohishi, "Characterization of an all-solid disordered tellurite glass optical fiber and its NIR optical image transport," Jpn. J. Appl. Phys, Vol. 58, pp. 032005 (1-8), 2019.

[17] K. Ito and J-i. Sakai, "Comparative study of direct image transmission through various optical fibers using the phase-conjugate wave," Jpn. J. Appl. Phys. Vol. 46, pp. 5172–5177, 2007.

[18] M. Sasaki, T. Ando, S. Nogawa, and K. Hane, "Direct photolithography on optical fiber end," Jpn. J. Appl. Phys. Vol. 41, pp. 4350–4355, 2002.

[19] S. Taue, Y. Matsumoto, H. Fukano, and K. Tsuruta, "Experimental analysis of optical fiber multimode interference structure and its application to refractive index measurement," Jpn. J. Appl. Phys. Vol. 51, pp. 04DG14 (1-4), 2012.

[20] M. Ohki, N. Shima, and T. Shiosaki, "Measurement of piezoelectric vibration using optical fiber," Jpn. J. Appl. Phys. Vol. 31, pp. 105-107 1992.

[21] P.D. Dragic, M. Cavillon, and J. Ballato, "Materials for optical fiber lasers: A review," Appl. Phys. Rev. Vol. 5, pp. 041301 (1-37), 2018.

[22] B.E.A. Saleh and M.C. Teich, *Fundamentals of Photonics*, Wiley, New Jersey, 2007.

[23] M. Tateda and M. Ikeda, "Mode conversion in bent step index multimode fibers," Appl. Optics, Vol. 15, No. 10, pp. 2308-2310, 1976.

[24] R.A. Potyrailo, V.P. Ruddy, and G.M. Hieftje, "Kramers–Kronig analysis of molecular evanescent-wave absorption spectra obtained by multimode step-index optical fibers," Appl. Optics, Vol. 35, No. 21, pp.4102-4111, 1996.

[25] B.S. Kawasaki and K.O. Hill, "Low-loss access coupler for multimode optical fiber distribution networks," Appl. Optics, Vol. 16, No. 7, pp.1794-1795, 1977.

[26] D.R. Gabardi and D.L. Shealy, "Coupling of domed light-emitting diodes with a multimode step-index optical fiber," Appl. Opt. Vol. 25, No. 19, pp.3435-3442, 1986.

[27] S. Morris, C. McMillen, T. Hawkins, P. Foy, J. Ballato, and R. Rice, "The influence of core geometry on the crystallography of silicon optical fiber," J. Cryst. Growth, Vol. 352, No. 1, pp.53-58, 2012.

[28] F.M. Dickey, S.C. Holswade, and D.L. Shealy, *Laser Beam Shaping Applications,* CRC Press, 2005.

[29] O. Blomster and M. Blomqvist, "Square formed fiber optics for high power applications," in Proc. 4th Int. WLT-Conf. Lasers, 5, 2007.

[30] F. Schuberts, A. Hoben, K. Bakhshpour, and C. Provost, "Square fibers solve multiple application challenges," Photonic Spectra, Vol. 45, No. 2, pp.38-41, 2011.

[31] Y. Yan, L. Zhang, J. Wang, J-Y. Yang, I.M. Fazal, N. Ahmed, A.E. Willner, and S.J. Dolinar, "Fiber structure to convert a Gaussian beam to higherorder optical orbital angular momentum modes," Opt. Lett. Vol. 37, No. 16, pp.3294-3296, 2012.

[32] Z. Xiong, W. Chen, P. Wang, and Y. Chen, "Classification of symmetry properties of waveguide modes in presence of gain/losses anisotropy/bianisotropy, or continuous/discrete rotational symmetry," Opt. Exp., Vol. 25, No. 24, pp.29822-29834, 2017.

[33] T.E. Lizotte, "Laser beam uniformity and stability using homogenizer based fiber optic launch method: Square core fiber delivery," in Proc. Spie. Optical Fibers, 78940Y, 2011.

[34] H. Pakarzadeh, S.M. Rezaei, M. Taghizadeh and F. Bozorgzadeh, "Dispersion properties of single-mode optical fibers in telecommunication region: poly (methyl methacrylate) (PMMA) versus silica," J. Opt. Commun. doi.org/10.1515/joc-2020-0172.

[35] C.A. Balanis, *Advanced Engineering Electromagnetics*, Wiley, New York, 1989.

[36] A. Yariv and P. Yeh, Photonics: Optical Electronics in Modern Communications, Oxford University Press, 2007.

[37] O.V. Butov, K.M. Golant, A.L. Tomashuk, A.H.E. Breuls, and M.J.N. Stralen, "Refractive index dispersion of doped silica for fiber optics," Opt. Commun, Vol. 213, No. 4-6, pp. 301-308, 2002.

[38] R. Kitamura, L. Pilon, and M. Jonasz, "Optical constants of silica glass from extreme ultraviolet to far infrared at near room temperature," Appl. Opt. Vol. 46, No. 33, pp. 8118-8133, 2007.

[39] H.S. Nalwa, Silicon-Based Materials and Devices 2, Academic Press, 2001.

[40] L. Mousavi, M. Sabaeian, and H. Nadgaran, "Thermally-induced birefringence in solid-core photonic crystal fiber lasers," Opt. Commun. Vol. 300, pp. 69-76, 2013.

[41] J. Van de Casteele, M. Bettiati, F. Laruelle, V. Cargemel, P. Pagnod-Rossiaux, P. Garabedian, L. Raymond, D. Laffitte, S. Fromy, D. Chambonnet, and J.P. Hirtz, "High reliability level on single-mode 980 nm-1060 nm diode lasers for telecommunication and industrial applications," Proc. SPIE 6876, High-Power Diode Laser Technology and Applications VI, 68760P, 2008.

[42] A. Pietrzak, M. Zorn, R. Huelsewede, J. Meusel, and J. Sebastian, "Development of highly efficient laser diodes emitting around 1060nm for medical and industrial applications," Proc. SPIE10900, High-Power Diode Laser Technology XVII, 109000K, 2019.

[43] M. Bettiati, F. Laruelle, V. Cargemel, P. Bourdeaux, P. Pagnod-Rossiaux, P. Garabedian, J. Van de Casteele, S. Fromy, D. Chambonnet, and J. P. Hirtz, "High brightness single-mode 1060-nm diode lasers for demanding industrial applications," Proc. CLEO/Europe and IQEC, pp. CB. 19, 2007.

[44] P. Dupriez, A. Piper, A. Malinowski, J.K. Sahu, M. Ibsen, B.C. Thomsen, Y. Jeong, L.M.B. Hickey, M.N. Zervas, J. Nilsson, and D.J. Richardson, "High average power, high repetition rate, picosecond pulsed fiber master oscillator power amplifier source seeded by a gain-switched laser diode at 1060 nm," IEEE Photon. Technol. Lett. Vol. 18, pp. 1013-1015, 2006.

[45] M.J. Miah, T. Kettler, K. Posilovic, V.P. Kalosha, D. Skoczowsky, R. Rosales, D. Bimberg, J. Pohl, and M. Weyers, "1.9 W continuous-wave single transverse mode emission from 1060 nm edge emitting lasers with vertically extended lasing area," Appl. Phys. Lett. Vol. 105, pp. 151105 (1-5), 2014.

[46] J. Mi, H. Yu, H. Wang, S. Tan, W. Chen, Y. Ding, and J. Pan, "A GaAs-based hybrid integration of a tunneling diode and a 1060-nm semiconductor laser," IEEE Photon. Technol. Lett. Vol. 27, pp. 169-172, 2015.

[47] M. Kuznetsov, W. Atia, B. Johnson, and D. Flanders, "Compact ultrafast reflective Fabry-Perot tunable lasers for OCT imaging applications," Proc. Spie. Optical Coherence

Tomography and Coherence Domain Optical Methods in Biomedicine, Vol. 7554, pp. 75541F (1-6), 2010.

[48] R. Kaufmann, A. Hartmann and R. Hibst, "Cutting and skin-ablative properties of pulsed mid-infrared laser surgery," J. Dermatol. Surg. Oncol, Vol. 20, pp. 112-118, 1994.

[49] J. Malchus, V. Krause, G. Rehmann, M. Leers, A. Koesters, and D.G. Matthews, "A 40kW fiber-coupled diode laser for material processing and pumping applications," Proc. SPIE 9348, High-Power Diode Laser Technology and Applications XIII, 934803, 2015.

[50] G. Matthäus, T. Schreiber, J. Limpert, S. Nolte, G. Torosyan, R. Beigang, S. Riehemann, G. Notni, and A. Tünnermann, "Surface-emitted THz generation using a compact ultrashort pulse fiber amplifier at 1060 nm," Vol. 261, pp. 114-117, 2006.

[51] Z. Saghi, "Investigation of magnetic energy density for fundamental mode of square-core optical fiber," In Proc. 4th Conf. Computational. Phys. Tehran, pp. 67-70, 2020.

Zahra Saghi was born in Ahvaz, Iran, in 1996. She received the B.Sc degree in Physics, in 2017 from the Shahid Chamran University of Ahvaz. Then, she received her Master's degree in fundamental physics from the Shahid Chamran University of Ahvaz, in 2020.

In 2020, She joined the Department of Physics, Shahid Chamran University of Ahvaz, as an Assistant of Research. During her university studies, she was recognized and honored several times as a top talented student. Now, she is a member of the Physics Society of Iran. Her current research interests include light-matter interactions and optical fibers.